Petrunin, A., Meneses Rioseco, E., Sobolev, S. V., Weber, M. (2012): Thermomechanical model reconciles contradictory geophysical observations at the Dead Sea Basin. - Geochemistry Geophysics Geosystems (G3), 13, Q04011

DOI: 10.1029/2011GC003929

Geochemistry Geophysics Geosystems G3

Article
Volume 13, Number 4
28 April 2012
Q04011, doi:10.1029/2011GC003929
ISSN: 1525-2027

Published by AGU and the Geochemical Society

Thermomechanical model reconciles contradictory geophysical observations at the Dead Sea Basin

Alexey G. Petrunin
Helmholtz Centre Potsdam, GFZ German Research Centre for Geosciences, Telegrafenberg, D-14473 Potsdam, Germany

Schmidt Institute of Physics of the Earth, B. Gruzinskaya 10, 123995 Moscow, Russia (alexei@gfz-potsdam.de)

Ernesto Meneses Rioseco
Helmholtz Centre Potsdam, GFZ German Research Centre for Geosciences, Telegrafenberg, D-14473 Potsdam, Germany

Now at Leibniz Institute for Applied Geophysics, Stilleweg 2, D-30655 Hannover, Germany

Stephan V. Sobolev
Helmholtz Centre Potsdam, GFZ German Research Centre for Geosciences, Telegrafenberg, D-14473 Potsdam, Germany

Schmidt Institute of Physics of the Earth, B. Gruzinskaya 10, 123995 Moscow, Russia

Michael Weber
Helmholtz Centre Potsdam, GFZ German Research Centre for Geosciences, Telegrafenberg, D-14473 Potsdam, Germany

Institute of Earth and Environmental Science, University of Potsdam, Potsdam, Germany

[1] The Dead Sea Transform (DST) comprises a boundary between the African and Arabian plates. During the last 15–20 m.y. more than 100 km of left lateral transform displacement has been accumulated on the DST and about 10 km thick Dead Sea Basin (DSB) was formed in the central part of the DST. Widespread igneous activity since some 20 Ma ago and especially in the last 5 m.y., thin (60–80 km) lithosphere constrained by seismic data and absence of seismicity below the Moho, seem to be quite natural for this tectonically active plate boundary. However, surface heat flow values of less than 50–60 mW/m^2 and deep seismicity in the lower crust (deeper than 20 km) reported for this region are apparently inconsistent with the tectonic settings specific for an active continental plate boundary and with the crustal structure of the DSB. To address these inconsistencies which comprise what we call the "DST heat-flow paradox," we have developed a numerical model that assumes an erosion of initially thick and cold lithosphere just before or during the active faulting at the DST. The optimal initial conditions for the model are defined using transient thermal analysis. From the results of our numerical experiments we conclude that the entire set of observations for the DSB can be explained within the classical pull-apart model assuming that the lithosphere has been thermally eroded at about 20 Ma and the uppermost mantle in the region have relatively weak rheology consistent with experimental data for wet olivine or pyroxenite.

Components: 8200 words, 8 figures, 1 table.

Keywords: heat flow; pull-apart basin; tectonophysics; thermomechanical modeling; transform fault.

Index Terms: 0545 Computational Geophysics: Modeling (1952, 4255, 4316); 8111 Tectonophysics: Continental tectonics: strike-slip and transform; 8169 Tectonophysics: Sedimentary basin processes.

Received 19 October 2011; **Revised** 20 March 2012; **Accepted** 20 March 2012; **Published** 28 April 2012.

Petrunin, A. G., E. Meneses Rioseco, S. V. Sobolev, and M. Weber (2012), Thermomechanical model reconciles contradictory geophysical observations at the Dead Sea Basin, *Geochem. Geophys. Geosyst.*, *13*, Q04011, doi:10.1029/2011GC003929.

1. Introduction

[2] The Dead Sea Transform (DST) was formed as a result of the mid-Cenozoic break-up of the Arabian-Nubian platform, which was divided into the African and Arabian plates. During the last 15–20 m.y. more than 100 km of left lateral transform displacement has been accumulated on the DST [*Garfunkel and Ben-Avraham*, 1996]. Owing to a number of recent international geophysical studies [e.g., *Weber et al.*, 2004, 2009; *ten Brink et al.*, 2006; *Mechie et al.*, 2009; *Chang and Van der Lee*, 2011], the lithospheric structure in the region is well studied. These observations (see details below) infer that lithosphere in the region is thin, what seems to be quite natural for an active plate boundary. This view of the DST, however, contradicts surface heat flow data of less than 50–60 mW/m^2 [*Eckstein and Simmonsi*, 1977; *Eckstein*, 1978; *Shalev et al.*, 2008] and deep seismicity in the lower crust [*Aldersons et al.*, 2003; *Shamir*, 2006] (see details below) reported for this region. This inconsistency, which comprises what we call the "DST heat-flow paradox," applies also for the more than 10 km thick Neogene Dead Sea Basin (DSB), located directly at the DST. This basin has long been considered a classical pull-apart structure [e.g., *Garfunkel and Ben-Avraham*, 1996]. However, recently *Ben-Avraham and Schubert* [2006] and *Ben-Avraham et al.* [2010] dismissed a pull-apart origin for the deepest southern part of the DSB. Among the major arguments was again the apparently anomalously cold crust of the DSB based on measured surface heat flow values below 50 mW/m^2 and unusually deep seismicity, persisting into the lower crust. Indeed numerical thermomechanical models [*Petrunin and Sobolev*, 2006, 2008] suggest that the formation of a pull-apart basin is likely impossible in the lithosphere with steady state surface heat flow below 50 mW/m^2 because in such a lithosphere the entire crust is rheologically strong and is mechanically attached to the even stronger upper mantle.

[3] In this study we use a 3D thermomechanical modeling technique to address the "DST heat-flow paradox," focusing on the origin of the DSB. We show that the observed surface heat flow, crustal structure and distribution of seismicity in the lithosphere below the basin can be reconciled with the pull-apart origin of the DSB. Along with the shear heating effect at the faults and ductile part of the lithosphere, the key issue is the transient thermal state of the lithosphere caused by lithospheric thinning that took place in the region prior to or during the first stage of the formation of the DSB at about 15–20 Ma.

2. The Dead Sea Basin (DSB)

[4] The DSB was formed at the left-lateral overstepping of the Dead Sea Transform during continuous sinistral displacement along the DST, accommodating about 100 km offset between the Arabian plate and the Sinai microplate since Middle Miocene [*Quennell*, 1958; *Freund et al.*, 1970; *Bartov et al.*, 1980; *Garfunkel*, 1981]. The basin is characterized by a sedimentary layer thickness of about 10–12 km and a length around 150 km, whereas the width of the basin is only 12–15 km [*Garfunkel and Ben-Avraham*, 1996]. The shape of the basin in combination with a structure of steep bounding faults have led to different definitions of the DSB such as "rift valley," "trough," "graben," "pull-apart basin" [e.g., *Garfunkel*, 1981; *Ben-Avraham and Zoback*, 1992], or even "drop down basin" [*Ben-Avraham and Schubert*, 2006].

[5] Compilation of gravity, magnetic [*ten Brink et al.*, 1993; *Rybakov et al.*, 1997; *Götze et al.*, 2007; *Segev et al.*, 2006], seismic tomography data [*Hofstetter et al.*, 2000; *Koulakov and Sobolev*, 2006; *Koulakov et al.*, 2006] as well as several seismic profiles crossing the DSB area [*Weber et al.*, 2004; *ten Brink et al.*, 2006; *Mechie et al.*, 2009] provide detailed information on the crustal structure of the region. These data suggest that the

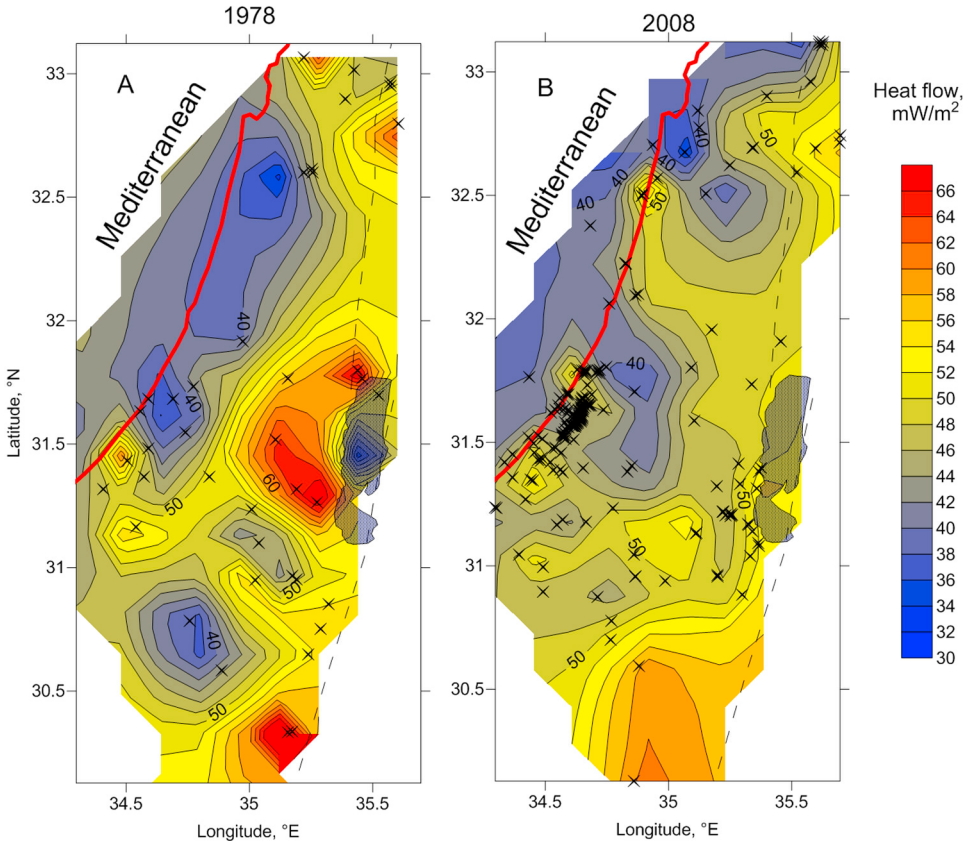

Figure 1. Surface heat flow distribution at the DST area according to data from *Eckstein and Simmonsi* [1977] and *Ben-Avraham et al.* [1978]. (a) From compilation of *Pollack et al.* [1993] and (b) after *Shalev et al.* [2008]. For Figure 1a, 10% of the least characteristic data are not included (surface heat flow values lower than 25 mW/m^2 and higher than 80 mW/m^2). Black crosses indicate measuring sites.

crust to the west of the DST is of a transitional type between the covered by Mesozoic sediments oceanic crust of the Eastern Mediterranean (about 20 km thick), and the 40 km thick continental crust of the Arabian Shield. These data also indicate a 32 km thick crust at the DSB area that is somewhat thinner than the average continental crust. Interestingly, both seismic profiles [*ten Brink et al.*, 2006; *Mechie et al.*, 2009] show neither significant uplift of the Moho, as it is expected for the classical rift structure, nor flexure at the upper-lower crustal boundary, despite the strongly extended upper crust. This indicates that severe deformation that led to the formation of the DSB was almost completely limited to the upper 20 km of the crust.

2.1. Is the Lithosphere at the DSB Hot or Cold?

[6] Geophysical data, collected for the DSB region to date, give contradictory interpretations of the thermal state of the lithosphere. The heat flow data for the region argue in favor of a rather cold lithosphere. As mentioned above, surface heat flow values lower than 50 mW/m^2 has been reported for Israel (Figure 1) [*Eckstein and Simmonsi*, 1977; *Eckstein*, 1978; *Shalev et al.*, 2008]. These values are more appropriate for Archean rather than Neoproterozoic lithosphere and assume thick cold continental lithosphere. Measurements at the water area of the Dead Sea [*Ben-Avraham et al.*, 1978] also indicate extremely low surface heat flow (about 30 mW/m^2), which can be explained, however, by active groundwater circulation. The fluid downward advection may significantly reduce the value of surface heat flow at downstream filtration areas and, contrary, increase the value at the flanks of the DSB, where the heated water comes out to the surface [*Shalev et al.*, 2007]. Such a coupled anomaly is clearly seen in Figure 1a to the west of the Dead Sea. The recent study in southern Israel [*Schütz et al.*, 2012] shows a possible surface heat flow range of 55–60 mW/m^2 and suggests that previously reported lower values for the entire region might have been biased. There are only few data on the surface heat flow in Jordan. *Galanis et al.* [1986] report exceedingly high surface heat

flow (>400 mW/m^2) to the east of the Dead Sea, which can also be explained by discharging of a hot groundwater in the region. After discarding these high values, the surface heat flow in Jordan varies from 42 to 65 mW/m^2 [*Galanis et al.*, 1986] and has a mean value close to 60 mW/m^2 [*Förster et al.*, 2007]. Thus, after filtering extreme values, the surface heat flow in the region has a clear tendency to decrease toward the Mediterranean cost (to values of about 40 mW/m^2) and to increase toward the Red Sea to values higher than 60 mW/m^2 (Figure 1).

[7] Summing up the heat flow data we conclude that in the DSB area, the mean surface heat flow is about 50–53 mW/m^2 corresponding to a lithospheric thickness of more than 130 km, but it may be in fact somewhat higher (say 57 mW/m^2) if the suggestion about underestimation of the surface heat flow by earlier measurements [*Schütz et al.*, 2012] is correct. For the modeling we mostly rely on the estimate of 50–53 mW/m^2, but we will also consider the possibility of higher (57 mW/m^2) surface heat flow values.

[8] Another evidence for a cold lithosphere in the study area is the unusual for Neoproterozoic lithosphere seismicity pattern at the DSB. As reported by *Aldersons et al.* [2003], 60 percent of the micro-earthquakes are located at depths of about 20–32 km (lower crust) and the peak seismicity is situated just below the upper-lower crustal boundary (at 20 km depth). A more recent study, based on the double difference relative relocation method, suggests that the seismic activity at the DSB is mostly confined to the upper crust (0–20 km), but also confirms significant seismicity between 20 and 25 km depth [*Shamir*, 2006]. The seismicity in the lower crust indicates its low temperature and brittle rheology in accord with the low surface heat flow reported for this area [*Ben-Avraham and Lazar*, 2006].

[9] However, there also exists geophysical evidence suggesting thin and hot lithosphere at the DSB. The present-day lithospheric thickness of about 60–80 km is revealed by receiver-functions analyses [*Mohsen et al.*, 2006], which is notably less than expected for the lithosphere based on its age [*Artemieva and Mooney*, 2001]. Thin lithosphere beneath the DST and surroundings is also confirmed by anomalously low seismic velocities in the mantle deeper than 50–70 km detected by recent seismic tomography studies [*Chang and Van der Lee*, 2011; *Chang et al.*, 2011]. Additionally, the local earthquakes data show no seismic activity in the mantle lithosphere [*Aldersons et al.*, 2003; *Shamir*, 2006]. The fact of absence of earthquake sources beneath the Moho could indicate a ductile material flow assuming rather high temperatures of the mantle lithosphere. Moreover, two seismic profiles crossing the DSB area [*ten Brink et al.*, 2006; *Mechie et al.*, 2009] show no prominent topography both at the Moho, as it is expected for the classical rift structure, and at the upper-lower crustal boundary, despite the strongly extended upper crust. This can be explained by relatively weak crustal rheology, allowing either compensating material flow in the lower crust [*Al-Zoubi and ten Brink*, 2002] or, more likely, decoupling of deformation at the mid-crustal level, such that intensive fault-parallel extension was entirely localized in the upper brittle part of the crust [*Petrunin and Sobolev*, 2006, 2008]. Both of these processes are inconsistent with the cold lithosphere.

2.2. Could the Afar Plume Influence the Lithosphere Beneath DST?

[10] Recent tomographic imaging of velocity structure beneath Arabia and surroundings, based on joint inversion of S- and SKS arrival times, S- and Rayleigh waveform fits and compilation of other available data [*Chang and Van der Lee*, 2011; *Chang et al.*, 2011], has revealed new evidence for one or more mantle plumes that pumped hot material beneath Arabia and in particular the area of low seismic velocities beneath the DST. They also suggest that southward mantle flow from the Jordan plume in combination with northward mantle flow from the Afar plume may be responsible for the extensive volcanism in western Arabia. These assumptions are also supported by Rayleigh wave tomography and shear wave splitting studies, showing channeled horizontal mantle flow from Afar plume oblique to the Red Sea rift axis [*Hansen et al.*, 2006, 2007; *Park et al.*, 2007, 2008].

[11] Plume-related magmatic activity started at about 20 Ma in the DST region [*Krienitz et al.*, 2009], which may indicate the arrival of the plume. Interestingly, there is no evidence for the kilometer-scale uplift in the central and northern part of the DST at that time [*Garfunkel and Ben-Avraham*, 1996; Z. Garfunkel, personal communication, 2012], the uplift that would be expected if thermal mantle plume impinged on the base of the lithosphere [e.g., *Farnetani and Richards*, 1994]. This contradiction can be resolved assuming that the plume was in fact thermo-chemical, rather than thermal, and it had high content of heavy recycled

oceanic crust, as recently suggested for the plume that generated the Siberian traps at 252 Ma [*Sobolev et al.*, 2011]. Such a plume has almost neutral buoyancy and therefore does not produce significant surface uplift. Much smaller scale of magmatic activity in Arabia than for the Siberian traps was likely due to smaller plume volume and/or lower excess temperature, i.e., less than 200°C for the plume beneath Arabia [*Krienitz et al.*, 2009] versus 250°C [*Sobolev et al.*, 2011] or even 300°C [*Sobolev et al.*, 2009] for the Siberian plume. Note that our hypothesis may be tested by analyzing compositions of magnesium-rich olivines from the Jordanian and Syrian basalts. If our hypothesis is correct, then the olivines must have high content of Ni and low Mn/Fe ratio, similar to the olivines from the Hawaiian basalts [*Sobolev et al.*, 2005b].

[12] Thermo-chemical plume may cause erosion of the lithosphere in less than few million years [*Sobolev et al.*, 2011]. Our model suggests that erosion of 60 to 80 km of the lower part of the thermal lithosphere should cause uplift of 0.3–0.5 km. Data on paleo-elevation in the DST region is incomplete and needs more analysis (Z. Garfunkel, personal communication, 2012). However, there is indication that uplift of 0.5 km or even higher indeed took place at about 20 Ma in the southern part of the DST (region of the present Gulf of Aqaba and southern Jordan), while similar uplift of the DSB shoulders perhaps took place later, since some 10 Ma ago [*Garfunkel and Ben-Avraham*, 1996; Z. Garfunkel, personal communication, 2012].

[13] Based on the above considerations we suggest that hot thermo-chemical plume that arrived at the DST region at about 20 Ma caused mechanical instability of the lowermost lithosphere, resulting in lithospheric erosion between 20 and 10 Ma. According to this scenario, the uppermost lithosphere remained close to its initial thermal state till present-day, whereas its lower part underwent a noticeable heating.

3. Numerical Models

3.1. 1D Transient Thermal Analysis

[14] At the first stage we implemented a simple 1D numerical transient thermal model to test the idea of instant lithospheric erosion as a possible explanation for the contradictory geophysical observations. First, we solve a two boundary value problem to find initial steady state geotherms for the range of thermal lithospheric thicknesses of 120–180 km. The surface and bottom temperatures are fixed and equal to 0°C and 1350°C, respectively. We simulate then the instant lithospheric erosion by replacing the lower (deeper than 80 km) part of the lithosphere with the plume having a temperature of 1450°C and solve the transient thermal problem. The goal is to find possible ranges of two parameters, (i) the initial thickness of the lithosphere and (ii) time of lithospheric erosion, that would be consistent with the present-day surface heat flow (away from the fault zone) of 50–53 mW/m^2 and present-day temperature at the Moho (in the fault zone) of more than 600°C, where no earthquakes are expected in peridotite (see below). The model uses the thermal material properties, which were determined by *Förster et al.* [2010] for the DST region (Table 1). As shear heating has a significant impact on the temperature in an active fault zone [e.g., *Thatcher and England*, 1998; *Leloup et al.*, 1999], it was included in the model of the temperature evolution in the fault zone. The value of the shear heating term was estimated based on our previous 2.5D thermomechanical model [*Sobolev et al.*, 2005a], i.e., assuming that the 20 km wide zone of deformation at the DSB has an average strike-slip motion rate of 0.6 cm per year. This value was also confirmed later by the 3D thermomechanical models. However, for the calculation of the surface heat flow away from the fault zone where the deformation is insignificant, we neglected shear heating.

[15] As can be seen from Figure 2, the surface heat flow (solid curves show isolines of surface heat flow) remains unchanged during the first 10 m.y. after lithospheric erosion, whereas temperature at the Moho significantly grows after only few millions years. The change of the temperature at the Moho is controlled by two factors: (i) shear heating at and below the fault system and (ii) conductive heating due to erosion of the lower lithosphere. The first factor dominates and starts to act immediately whereas conductive heating of the Moho increases gradually with time (Figure 3). At about 20 m.y. after lithospheric erosion, the influence of both factors becomes comparable, especially for the models with initially thick (i.e., relatively cold) lithosphere.

[16] To be aseismic, rock deformation must be either ductile or frictional (brittle) with velocity strengthening behavior [*Dieterich*, 1979]. For the mantle peridotite, the transition from velocity weakening (seismic) to velocity strengthening (aseismic) behavior occurs at about 600°C [*Boettcher et al.*, 2007]. We therefore assume that the mantle lithosphere is aseismic at temperatures

Table 1. Material Parameters[a]

Parameter	Sediments	Upper Crust	Lower Crust	Mantle
Density, ρ (kg/m^3)	2300/2400	2750	2950	3250
Thermal expansion, $\alpha \times 10^5$ (K^{-1})	3.7	3.7	2.7	3.0
Elastic moduli, K; G (GPa)	55; 36	55; 36	63; 40	122; 74
Heat capacity, C_p (J/kg/K)	1200	1200	1200	1200
Heat conductivity, λ (W/K/m)	pressure-temperature dependent, see *Förster et al.* [2010]			
Heat productivity, A (μW/m^3)	0.8	1.48	0.03	0
Initial cohesion, C_h (MPa)	20	20	20	20
Strain softening: cohesion	70% at 0 to 10% strain	70% at 0 to 10% strain	70% at 0 to 10% strain	90% at 0 to 10% strain
Initial friction coefficient, μ	0.5	0.5	0.5	0.5
Strain softening: friction	80% at 10% to 50% strain		-	-
Pre-exponential constant for dislocation creep, log(B_n) (Pa^{-n} s^{-1})	−28.0 (1)	"strong"	"strong" −14.75 (2)	dry −15.2 (3)
		−28.0 (1)		wet −14.7 (3)
		"weak" −17.3 (4)	"weak" −22.68 (4)	
Power law exponent, n	4.0 (1)	"strong" 4.0 (1)	"strong" 3.0 (2)	3.5 (3)
		"weak" 2.3 (4)	"weak" 3.2 (4)	
Activation energy for dislocation creep, E_n (kJ/mol)	223 (1)	"strong" 223 (1)	"strong" 356 (2)	dry 530 (3)
		"weak" 154 (4)	"weak" 238 (4)	wet 480 (3)
Activation volume (cm^3)	0	"strong" 15 (1)	0	dry 13 (3)
		"weak" 0 (4)		wet 8 (3)

[a]Dislocation creep law parameters numbered in parentheses as follows: 1, *Gleason and Tullis* [1995]; 2, *Rybacki and Dresen* [2000]; 3, *Hirth and Kohlstedt* [2003]; 4, *Ranalli* [1995]. Source for diffusion and Peierls' creep laws in mantle: *Kameyama et al.* [1999]. For "weak" mantle models reduced reference Peierls' stress value (from 85 kbar to 40 kbar) is used.

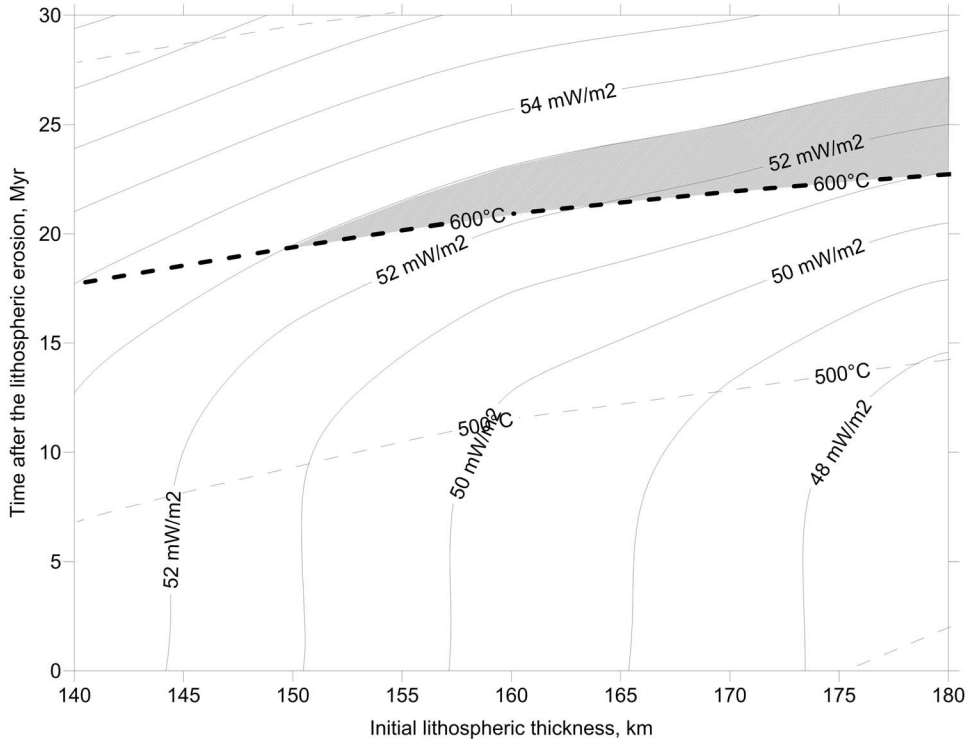

Figure 2. Time-evolution of the surface heat flow and temperature at the Moho. The temperature is adjusted so that shear heating is included. The thick dashed line marks the transition from seismic to aseismic deformation in the uppermost mantle lithosphere. All values are given for a thickness of lithosphere after thermal erosion of 80 km.

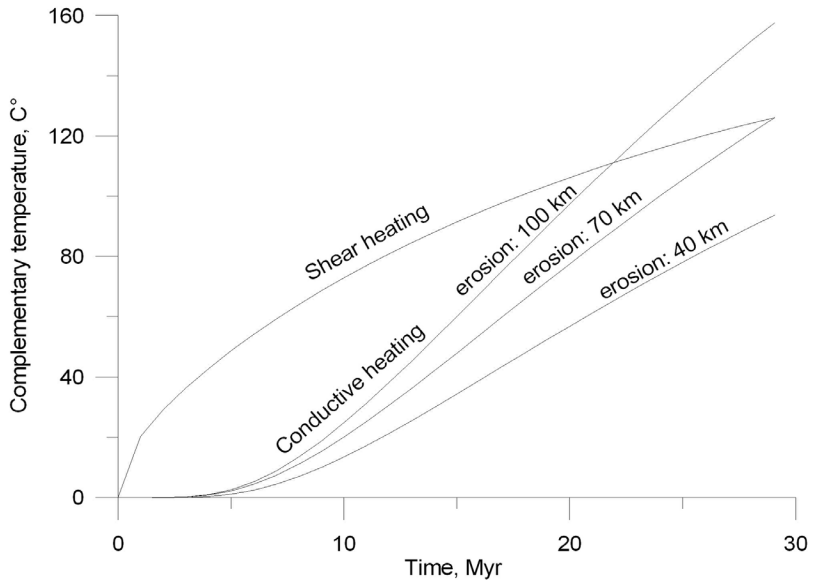

Figure 3. Temperature rise caused by shear heating and conductive heat transfer due to instant thermal erosion of the lithosphere at the Moho beneath a growing pull-apart basin.

above 600°C (thick dashed line in Figure 2), even if the operating deformation mode is brittle. Hatched domain in Figure 2 shows the range of parameters that fulfill both the temperature at the Moho (600°C) condition and the condition that surface heat flow must be between 50 and 53 mW/m^2. It is clear that both conditions mainly constrain the time after the lithospheric erosion that therefore should be between 16 and 25 million years. Note, however, that if rheology of mantle rocks allows them to deform in ductile mode at temperatures below 600°C, say at 500°C, then no earthquakes would take place in the mantle even 10 m.y. after the lithospheric erosion event.

[17] Thus, simple thermal analysis allows us to limit the range of models that formally satisfy some of the observations for the DST region. However, for a more detailed analysis that takes into account all available data as well as nonlinear lithospheric rheology, we perform a series of 3D thermomechanical simulations.

3.2. A 3D Thermomechanical Model

[18] 3D models of the long-term evolution of transform faults and related structures employing realistic rheology of the lithosphere [*Petrunin and Sobolev*, 2008; *Gerya*, 2010] are still very rare. We have designed a 3D thermomechanical model addressing the apparently contradicting observations mentioned above. The model has structural and tectonic settings similar to the Dead Sea basin and considers it as a classical pull-apart basin. The lithosphere includes three-layer continental crust, which consists of sediments, felsic upper crust and mafic lower crust with quartz- (sediments and upper crust) or plagioclase- (lower crust) dominated rheology and a peridotite mantle with olivine-dominated rheology (Figure 4). The initial temperature distribution is laterally uniform. To obtain an appropriate width and location of the pull-apart basin in primarily laterally homogeneous medium, we introduce two parallel weak seeds of faults in the upper crust with left-lateral offset of 12 km, where the friction coefficient is dropped to 0.1. The modeling domain is subjected to sinistral strike-slip motion with constant velocity of 0.6 cm/year, forcing the pull-apart basin to develop between two predefined faults nuclei. Similar to the 1D thermal model, the initial steady state geotherm is disturbed by replacing part of the lithosphere below 80 km with mantle material with a temperature of 1450°C, simulating instant lithospheric erosion by hot plume material at model time 0. After that we switch on strike-slip displacement and run models for 17 million years. The model takes into account sediment loading. Any depression is filled with sediments as it subsides to depths of more than −500 m.

[19] Since the dynamics of the system depends on both temperature and mechanical properties of the medium, we perform a set of numerical experiments varying both the initial thermal lithosphere thickness and the rheological properties of the

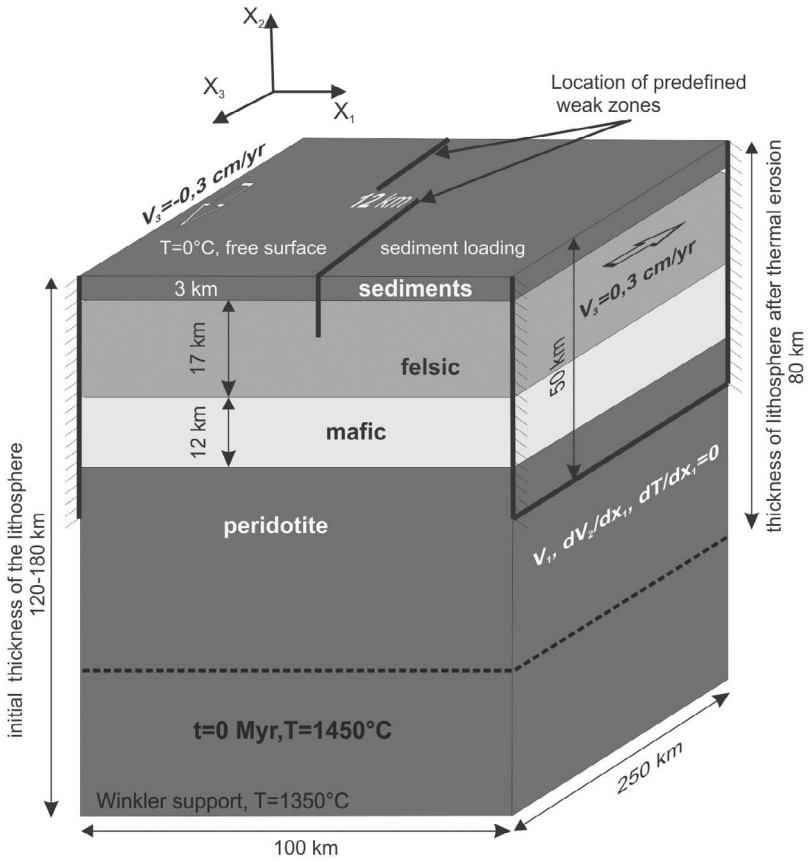

Figure 4. Setup of the 3D thermomechanical model. It is assumed that initially thick (120–180 km) lithosphere has been thermally eroded to 80 km at zero model time.

upper crust and upper mantle. The model set covers a range of initial thermal lithosphere thicknesses of 120–180 km, which correspond to the present-day surface heat flow at the basin shoulders of 50 mW/m^2 to 57 mW/m^2. All material properties of the model are given in Table 1.

[20] We model the thermomechanical evolution of the lithosphere, solving fully coupled three-dimensional conservation equations for momentum, mass and energy along with constitutive laws assuming visco-elasto-plastic rheology (see *Sobolev et al.* [2005a] and *Petrunin and Sobolev* [2008] for details). Brittle failure is simulated by Mohr-Coulomb friction rheology with a strain softening rule [*Huismans and Beaumont*, 2002; *Babeyko et al.*, 2002].

4. Results

[21] We have carried out a series of numerical experiments using different values for initial thermal thickness of the lithosphere and different rheological models of the upper crust and upper mantle. The aim of modeling was to determine whether there exist rheological models supported by experimental data that allow to fit the following set of observations for the DSB: (i) present-day surface heat flow at the DSB flanks of 50–53 mW/m^2 according to conservative estimate (see section 2.1) or 57 mW/m^2 based on new data [*Schütz et al.*, 2012], (ii) present-day lithospheric thickness of 80 km; (iii) thickness of Cenozoic sediments in the basin of 8–12 km; (iv) no prominent topography of the Moho and intracrustal boundary, (v) seismicity in the lower crust and (vi) no earthquakes in the mantle.

[22] The modeling results are presented in Figure 5, which show lithospheric structures at the model central cross-section after 105 km of strike-slip displacement. Figure 5 is organized as a table where the columns correspond to different initial thicknesses of the thermal lithosphere (or present-day surface heat flow) and the rows represent the different rheological models. As a proxy for the seismic activity we use the energy dissipation rate in the brittle (Mohr-Coulomb friction rheology)

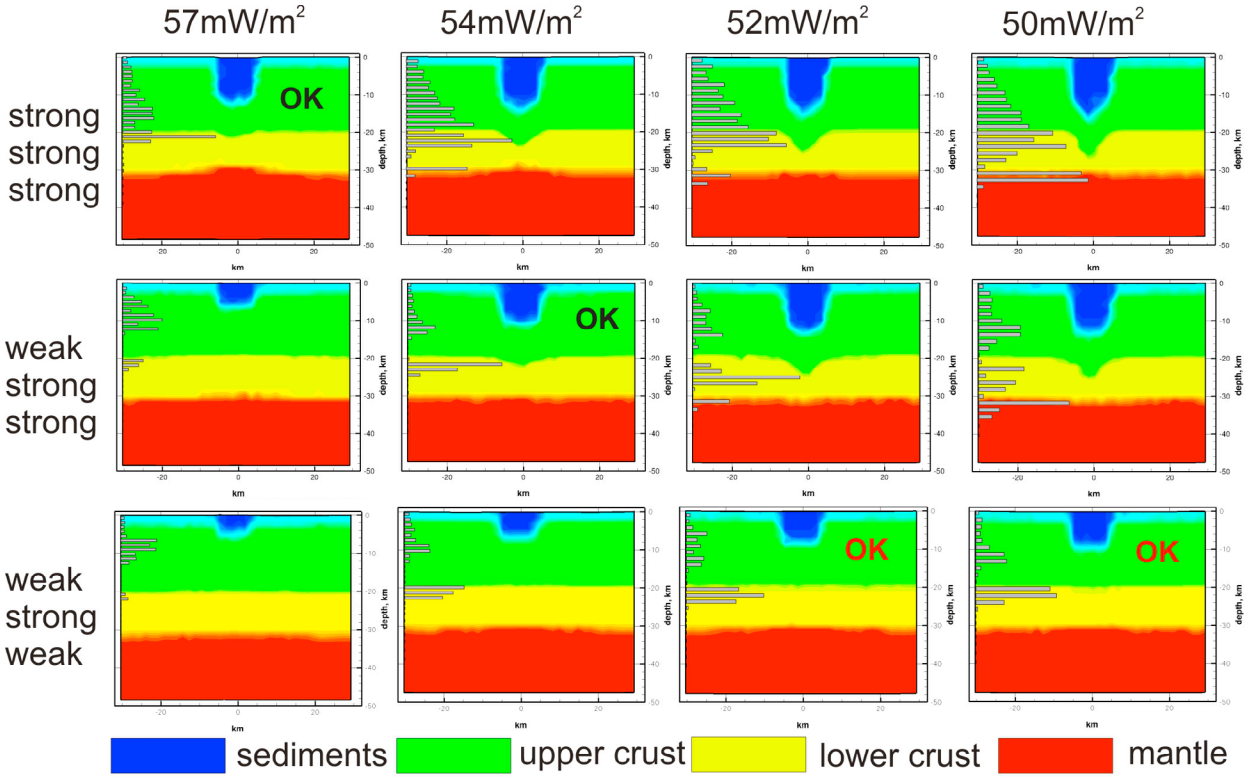

Figure 5. Lithospheric structures at the model central cross-section after 105 km of strike-slip motion for models with different initial lithospheric thickness and different rheology of the crust and mantle lithosphere. The columns correspond to the initial thermal lithosphere thicknesses of 120, 140, 160 and 180 km. Present-day surface heat flow values are indicated above each column. Horizontal bars show normalized mechanical energy dissipation rate in brittle ("seismic") regime. Numbers indicate predicted present-day (17 m.y. model time) surface heat flow at the flanks of the basin. Models which fit observations are marked with the "OK" text. Black labels denote the models with higher surface heat flow, consistent with recent data [*Schütz et al.*, 2012].

deformation mode. For the mantle we additionally assume that deformation is seismic provided the mantle lithosphere is brittle and it has temperature lower than 600°C [*Boettcher et al.*, 2007].

[23] The results show a clear trend of obtained deformation pattern depending on the model parameters. The rheological models with highest viscosities of both upper crust [*Gleason and Tullis*, 1995] and upper mantle [*Hirth and Kohlstedt*, 2003], shown in the top row of Figure 5, are not consistent with the conservative estimate of the surface heat flow at the DSB shoulders but agree well with the higher estimates [*Schütz et al.*, 2012]. These results are similar to our previous models [*Petrunin and Sobolev*, 2006, 2008]. If a lower-viscosity rheological model for the upper crust [*Ranalli*, 1995] is used (Figure 5, middle row), all the constraints are fulfilled for the model, which has still a slightly too high surface heat flow value (54 mW/m^2) than the conservative estimate. In the case where additionally the lower Peierls stress rheological model for the upper mantle is employed according to recent data by *Karato* [2008], the entire set of observational constraints is fitted even when the surface heat flow is as low as 50–52 mW/m^2 (Figure 5, bottom row). As demonstrated in Figure 6, modeling results do not change much if lithosphere is eroded at 25 Ma (Figure 6a) or at 9 Ma (Figure 6b) instead of 17 Ma (as in models presented in Figure 5).

[24] Finally, Figures 7 and 8 show the distribution of the dissipation rate in the brittle deformation mode (Figure 7) and corresponding strength envelopes at cross-sections of the center of the basin (Figure 8) for one of the low surface heat flow models that is consistent with the observations for the DSB. Figure 7 demonstrates that this dissipation rate, which we consider as a proxy for the seismicity, slowly moves upwards in the crust and decays with time, due to the heating of the lithosphere. Mechanical energy is dissipated also in the deep crust and in the mantle lithosphere down to a depth

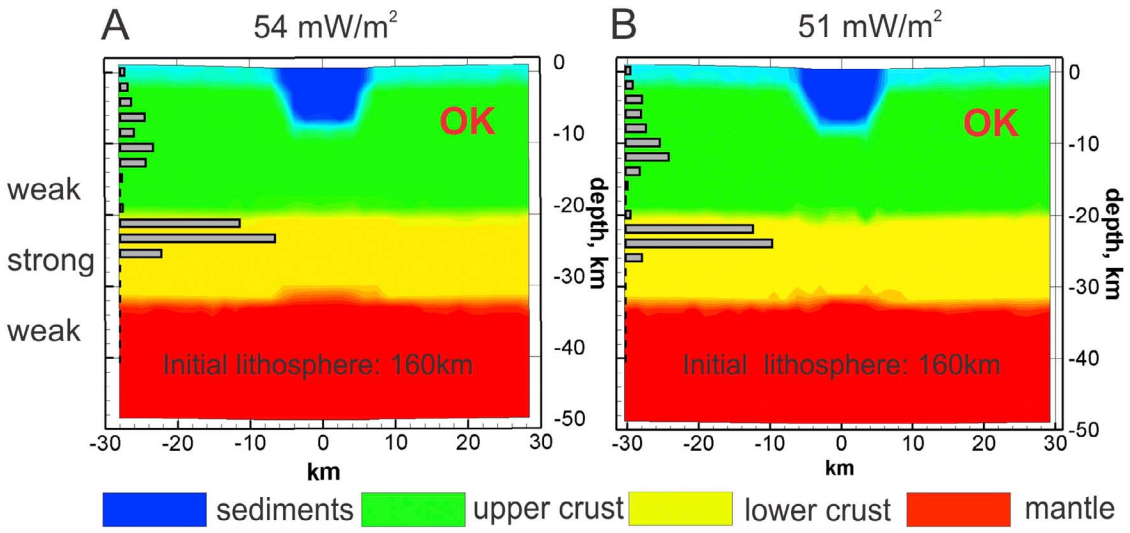

Figure 6. Lithospheric structure for the "best fit" models at the plain crossing the central part of the pull-apart basin after 105 km of strike-slip displacement. Lithospheric erosion was applied (a) 8 m.y. prior to (25 m.y. model time) and (b) 8 m.y. after (17 m.y. model time) the initiation of the strike-slip motion.

of about 60 km (Figure 7d), but in ductile deformation mode. We note that dissipation is concentrated in a zone with the width of about 20 km centered at the system of faults in accordance with the earlier modeling results [*Thatcher and England*, 1998; *Sobolev et al.*, 2005a]. Figure 8 shows how a zone of ductile decoupling is developed between lower crust and mantle lithosphere beneath the basin while lithosphere there heats up due to shear heating and heating through the base of the eroded lithosphere. Note also low friction in the upper crust that results from progressing strain softening.

5. Discussion and Conclusions

[25] The DSB, which is located directly at an active boundary between the African and Arabian plates, may be considered as an exceptional example of a natural rheological experiment. To be useful as a natural experiment, however, good knowledge of the style of deformation as well as internal structure and temperature distribution in the "specimen" is required. As the type of deformation at this plate boundary is predominantly strike-slip, the DSB is naturally considered in many studies as a classical strike-slip related subsidence structure, i.e., a pull-apart basin [e.g., *Garfunkel and Ben-Avraham*, 1996]. However, other hypotheses suggest a large rifting component at the DSB [*Ben-Avraham and Zoback*, 1992] as an important element of basin formation or consider the DSB as a "drop down" basin [*Ben-Avraham and Schubert*, 2006; *Ben-Avraham et al.*, 2010]. Recent high-resolution seismic studies [*ten Brink et al.*, 2006; *Mechie et al.*, 2009] have clearly shown that the entire stretching related to the DSB is localized in the upper part of the crust without any significant influence on the topography of the Moho and intracrustal boundaries. This crustal structure is consistent neither with a typical rift structure (where uplifted Moho is expected) nor with the expected crustal structure for the "drop down" basin (where subsided Moho is expected). The question is whether the observed crustal structure is consistent with the pull-apart model for the DSB, taking into account observed low surface heat flow in the region, and if the answer is "yes," what does it tell us about the rheology of the lithosphere in the region.

[26] From our 3D modeling we can clearly answer "yes" to the question raised above. The classical pull-apart model would work remarkably well for the DSB, without any additional assumption on the rheology of the lithosphere if two conditions were met (i) the lithosphere in the region was thinned/eroded in the time interval between 25 and 16 Ma and (ii) the present-day surface heat flow at the flanks of the DSB (after filtering away the effects of the circulation of fluids) was about 57 mW/m^2 as suggested by *Schütz et al.* [2012]. The surface heat flow, however, could not be significantly higher than 60 mW/m^2, since otherwise, isostatic uplift of the Moho would be expected [*Petrunin and Sobolev*, 2008].

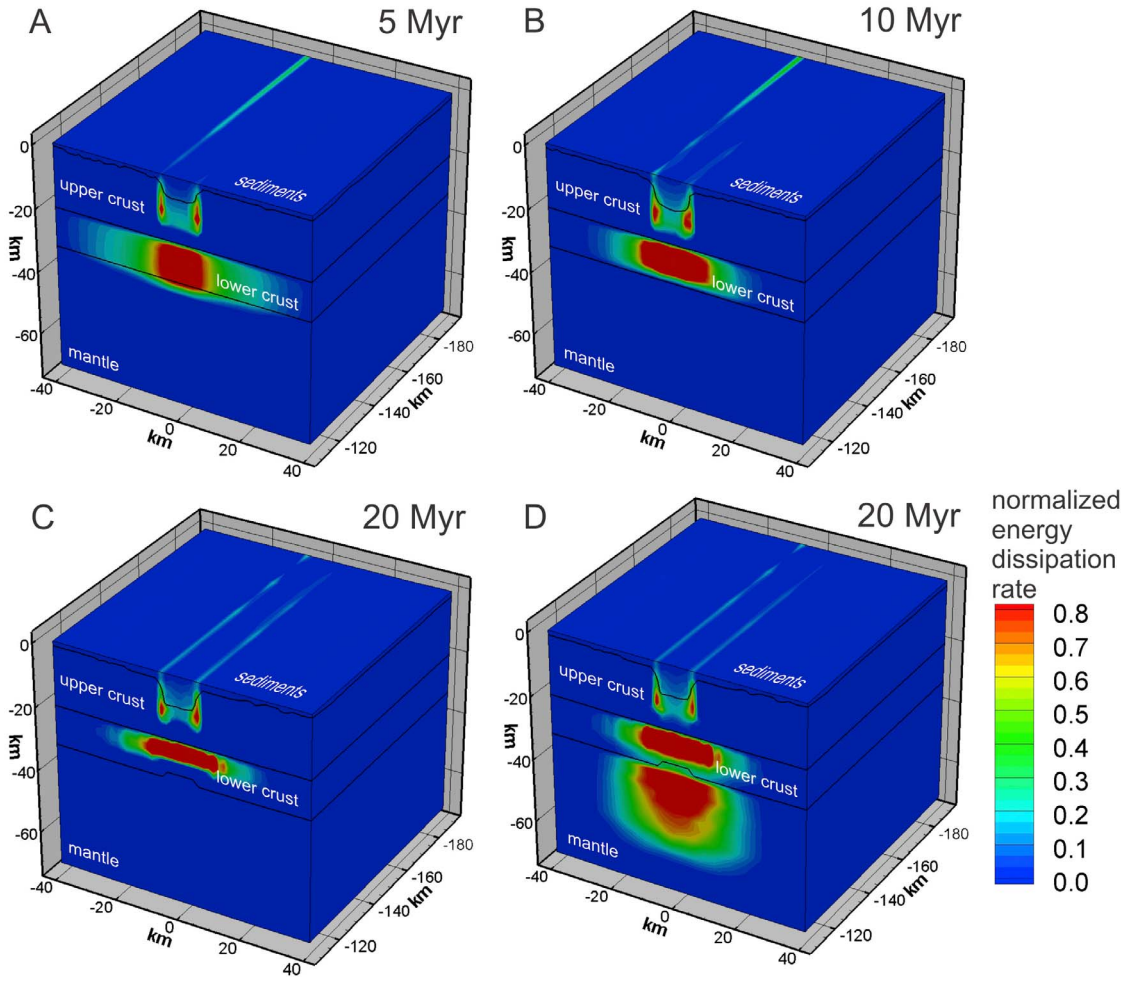

Figure 7. Crop of the modeling domain representing normalized energy dissipation rate within the pull-apart system. The front surface crosses the pull-apart basin at its center. (a–c) Brittle ("seismic") energy dissipation rate at 5, 10 and 20 m.y. model time for the "best fit" model (52 mW/m^2 surface heat flow at 17 m.y., weak rheology of both upper crust and lithospheric mantle and strong rheology of the lower crust. (d) Full energy dissipation rate for the same model at 20 m.y.

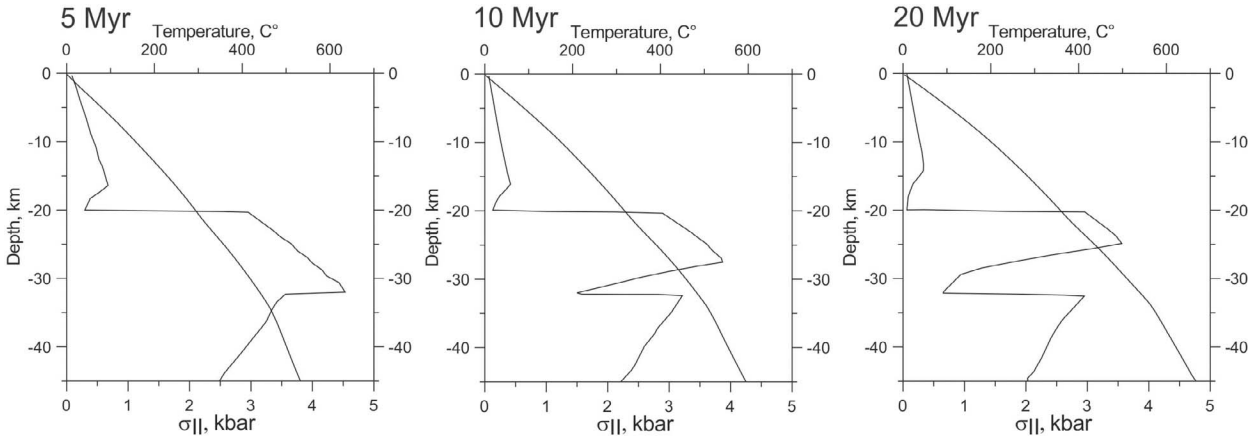

Figure 8. Temperature and strength over depth for the "best fit" model (52 mW/m^2 surface heat flow at 17 m.y., weak rheology of both upper crust and lithospheric mantle and strong rheology of the lower crust) at 5, 10 and 20 m.y. model time.

[27] The timing of the lithospheric erosion of 25–16 Ma ago is consistent with the data on the arrival of the plume beneath the Arabian plate region [*Krienitz et al.*, 2009] and the origination of the DST [*Garfunkel*, 1989, 1997]. Accompanied surface uplift in the southern part of the DST (up to 1 km high (Z. Garfunkel, personal communication, 2012)) is also consistent with such erosion if plume was thermo-chemical rather than purely thermal, and contained high amount of recycled oceanic crust [*Sobolev et al.*, 2011]. However, if at the DSB itself, significant uplift occurred later (at about 10 Ma) than in the southern part of the DST [*Garfunkel and Ben-Avraham*, 1996; Z. Garfunkel, personal communication, 2012], that may indicate that lithospheric erosion there also took place later, at around 10 Ma.

[28] If in fact the present-day surface heat flow at the DSB shoulders is only 50–53 mW/m^2 (conservative estimate) and lithospheric erosion took place at about 10 Ma, the model still can replicate the structure of the crust and seismicity pattern at the DSB if weaker than average rheology for the crust and upper mantle is considered. More specifically weak felsic rock rheology by *Ranalli* [1995] for the upper crust and relatively low Peierls stress for the lithospheric mantle based on recent laboratory experiments for wet olivine [*Karato*, 2008] proved to be sufficiently weak to explain all observations even for the present-day surface heat flow of about 50 mW/m^2 (Figure 5).

[29] We speculate that mantle lithosphere beneath the DST and surroundings might have been weakened by the water-containing fluids provided by a plume during its interaction with the initially thick lithosphere of the Arabian plate. Note that most of the mantle plumes contain significantly more water than MORB source mantle [*Dixon et al.*, 2002]. In addition, the presence of abundant orthopyroxene reported by *Stern and Johnson* [2010] in the lower crust and upper mantle in the study region might also contribute to the rheological weakening of these lithospheric domains. Laboratory experiments [e.g., *Skemer and Karato*, 2007; *Skemer et al.*, 2009] on orthopyroxene-rich rocks have shown a marked weakening of rocks under high strain. Skemer and co-authors [2009] suggest that orthopyroxene plays a critical role in shear localization. Interestingly, high content of pyroxene (>50%) in the uppermost mantle is perhaps not an unusual phenomenon as it was also suggested based on the interpretation of seismic data in Southern Germany [*Enderle et al.*, 1996]. Furthermore, weakening processes due to the grain size reduction in the high strain domains of the mantle and the crust at this plate boundary might also play a role [e.g., *Rutter and Brodie*, 1988; *Drury et al.*, 1991; *Hirth*, 2002].

[30] Finally, we note that the hypothesis of lithospheric erosion, together with the reasonable weakening of the lithospheric mantle allow to explain the absence of earthquakes in the mantle below the DST and DSB even in the case of surface heat flow of about 50–52 mW/m^2 (see Figure 5, bottom row). The key issue is the rise of the Moho temperature due to two processes, (i) energy dissipation during shear deformation (shear heating), and (ii) heating of the mantle lithosphere as a result of lithospheric erosion. Interestingly, our model suggests that few million years ago the Moho temperature below the DST and DSB was below 600°C and therefore seismicity in the mantle was possible. In general, our model predicts shallowing and slow decay of the seismicity in the region due to the heating of the lithosphere. This, however, does not take into account possible changes in plate velocities or additional factors like decrease of the water level in the Dead Sea.

[31] From our numerical experiments we conclude that the entire set of observational constraints for the DST and DSB including low surface heat flow of 50–60 mW/m^2, lithospheric thickness and crustal structure as well as seismicity pattern in the crust and absence of seismicity in the mantle can be explained with the predominantly strike-slip motion (DST) and classical pull-apart model (DSB) assuming that the lithosphere has been thermally eroded and mechanically weakened due to the interaction with a thermo-chemical mantle plume some 10–25 million years ago.

Acknowledgments

[32] A.G. Petrunin and E. Meneses Rioseco have been supported by the Deutsche Forschungsgemeinschaft in the framework of the DESIRE project and GeoForschungsZentrum Potsdam. We thank the DESIRE Group for providing data and helpful discussions during preparation of this manuscript. We also thank the Geological Survey of Israel and Eyal Shalev for providing the heat flow data for Israel. We extend our thanks to two anonymous reviewers for constructive comments on the manuscript.

References

Aldersons, F., Z. Ben-Avraham, A. Hofstetter, E. Kissling, and T. Al-Yazjeen (2003), Lower-crustal strength under the Dead Sea basin from local earthquake data and rheological

modeling, *Earth Planet. Sci. Lett.*, *214*(1–2), 129–142, doi:10.1016/S0012-821X(03)00381-9.

Al-Zoubi, A., and U. ten Brink (2002), Lower crustal flow and the role of shear in basin subsidence: An example from the Dead Sea basin, *Earth Planet. Sci. Lett.*, *199*(1–2), 67–79, doi:10.1016/S0012-821X(02)00540-X.

Artemieva, I. M., and W. D. Mooney (2001), Thermal thickness and evolution of Precambrian lithosphere: A global study, *J. Geophys. Res.*, *106*(B8), 16,387–16,414, doi:10.1029/2000JB900439.

Babeyko, A. Y., S. V. Sobolev, R. B. Trumbull, O. Oncken, and L. L. Lavier (2002), Numerical models of crustal scale convection and partial melting beneath the Altiplano–Puna plateau, *Earth Planet. Sci. Lett.*, *199*(3–4), 373–388, doi:10.1016/S0012-821X(02)00597-6.

Bartov, Y., G. Steinitz, M. Eyal, and Y. Eyal (1980), Sinistral movement along the Gulf of Aqaba—Its age and relation to the opening of the Red Sea, *Nature*, *285*(5762), 220–222, doi:10.1038/285220a0.

Ben-Avraham, Z., and M. Lazar (2006), The structure and development of the Dead Sea basin: Recent studies, in *New Frontiers in Dead Sea Paleoenvironmental Research*, edited by Y. Enzel, A. Agnon, and M. Stein, *Spec. Pap. Geol. Soc. Am.*, *401*, 1–13, doi:10.1130/2006.2401(01).

Ben-Avraham, Z., and G. Schubert (2006), Deep "drop down" basin in the southern Dead Sea, *Earth Planet. Sci. Lett.*, *251*(3–4), 254–263, doi:10.1016/j.epsl.2006.09.008.

Ben-Avraham, Z., and M. D. Zoback (1992), Transform-normal extension and asymmetric basins: An alternative to pull-apart models, *Geology*, *20*(5), 423–426, doi:10.1130/0091-7613(1992)020<0423:TNEAAB>2.3.CO;2.

Ben-Avraham, Z., R. Hanel, and H. Villinger (1978), Heat flow through the Dead Sea rift, *Mar. Geol.*, *28*(3–4), 253–269, doi:10.1016/0025-3227(78)90021-X.

Ben-Avraham, Z., V. Lyakhovsky, and G. Schubert (2010), Drop-down formation of deep basins along the Dead Sea and other strike-slip fault systems, *Geophys. J. Int.*, *181*(1), 185–197, doi:10.1111/j.1365-246X.2010.04525.x.

Boettcher, M. S., G. Hirth, and B. Evans (2007), Olivine friction at the base of oceanic seismogenic zones, *J. Geophys. Res.*, *112*, B01205, doi:10.1029/2006JB004301.

Chang, S.-J., and S. Van der Lee (2011), Mantle plumes and associated flow beneath Arabia and East Africa, *Earth Planet. Sci. Lett.*, *302*(3–4), 448–454, doi:10.1016/j.epsl.2010.12.050.

Chang, S.-J., M. Merino, S. Van der Lee, S. Stein, and C. A. Stein (2011), Mantle flow beneath Arabia offset from the opening Red Sea, *Geophys. Res. Lett.*, *38*, L04301, doi:10.1029/2010GL045852.

Dieterich, J. H. (1979), Modeling of rock friction: 1. Experimental results and constitutive equations, *J. Geophys. Res.*, *84*(B5), 2161–2168, doi:10.1029/JB084iB05p02161.

Dixon, J. E., L. Leist, C. Langmuir, and J.-G. Schilling (2002), Recycled dehydrated lithosphere observed in plume-influenced mid-ocean-ridge basalt, *Nature*, *420*(6914), 385–389, doi:10.1038/nature01215.

Drury, M. R., R. L. M. Vissers, D. Wal, and E. H. Hoogerduijn Strating (1991), Shear localisation in upper mantle peridotites, *Pure Appl. Geophys.*, *137*(4), 439–460, doi:10.1007/BF00879044.

Eckstein, Y. (1978), Review of heat flow data from the eastern Mediterranean region, *Pure Appl. Geophys.*, *117*(1–2), 150–159, doi:10.1007/BF00879742.

Eckstein, Y., and G. Simmonsi (1977), Measurement and interpretation of terrestrial heat flow in Israel, *Geothermics*, *6*(3–4), 117–142, doi:10.1016/0375-6505(77)90023-2.

Enderle, U., J. Mechie, S. Sobolev, and K. Fuchs (1996), Seismic anisotropy within the uppermost mantle of southern Germany, *Geophys. J. Int.*, *125*(3), 747–767, doi:10.1111/j.1365-246X.1996.tb06021.x.

Farnetani, C. G., and M. A. Richards (1994), Numerical investigations of the mantle plume initiation model for flood basalt events, *J. Geophys. Res.*, *99*(B7), 13,813–13,833, doi:10.1029/94JB00649.

Förster, A., H.-J. Förster, R. Masarweh, A. Masri, and K. Tarawneh (2007), The surface heat flow of the Arabian Shield in Jordan, *J. Asian Earth Sci.*, *30*(2), 271–284, doi:10.1016/j.jseaes.2006.09.002.

Förster, H.-J., A. Förster, R. Oberhänsli, and D. Stromeyer (2010), Lithospheric composition and thermal structure of the Arabian Shield in Jordan, *Tectonophysics*, *481*(1–4), 29–37, doi:10.1016/j.tecto.2008.11.014.

Freund, R., Z. Garfunkel, I. Zak, M. Goldberg, T. Weissbrod, B. Derin, F. Bender, F. E. Wellings, and R. W. Girdler (1970), The shear along the Dead Sea Rift [and discussion], *Philos. Trans. R. Soc. A*, *267*(1181), 107–130, doi:10.1098/rsta.1970.0027.

Galanis, S. P., J. H. Sass, R. J. Munroe, and M. Abu-Ajamieh (1986), Heat flow at Zerqa Ma'in and Zara and a geothermal reconnaissance of Jordan, *U.S. Geol. Surv. Open File Rep.*, *86-63*.

Garfunkel, Z. (1981), Internal structure of the dead sea leaky transform (rift) in relation to plate kinematics, *Tectonophysics*, *80*(1–4), 81–108, doi:10.1016/0040-1951(81)90143-8.

Garfunkel, Z. (1989), Tectonic setting of Phanerozoic magmatism in Israel, *Isr. J. Earth Sci.*, *38*, 51–74.

Garfunkel, Z. (1997), The history and formation of the Dead Sea basin, in *The Dead Sea: The Lake and Its Setting*, edited by T. M. Niemi et al., pp. 36–56, Oxford Univ. Press, New York.

Garfunkel, Z., and Z. Ben-Avraham (1996), The structure of the Dead Sea basin, *Tectonophysics*, *266*(1–4), 155–176, doi:10.1016/S0040-1951(96)00188-6.

Gerya, T. (2010), Dynamical instability produces transform faults at mid-ocean ridges, *Science*, *329*(5995), 1047–1050, doi:10.1126/science.1191349.

Gleason, G. C., and J. Tullis (1995), A flow law for dislocation creep of quartz aggregates determined with the molten salt cell, *Tectonophysics*, *247*(1–4), 1–23, doi:10.1016/0040-1951(95)00011-B.

Götze, H.-J., R. El-Kelani, S. Schmidt, M. Rybakov, M. Hassouneh, H.-J. Förster, and J. Ebbing (2007), Integrated 3D density modelling and segmentation of the Dead Sea Transform, *Int. J. Earth Sci.*, *96*(2), 289–302, doi:10.1007/s00531-006-0095-5.

Hansen, S., S. Schwartz, A. Al-Amri, and A. Rodgers (2006), Combined plate motion and density-driven flow in the asthenosphere beneath Saudi Arabia: Evidence from shear-wave splitting and seismic anisotropy, *Geology*, *34*(10), 869–872, doi:10.1130/G22713.1.

Hansen, S. E., A. J. Rodgers, S. Y. Schwartz, and A. M. S. Al-Amri (2007), Imaging ruptured lithosphere beneath the Red Sea and Arabian Peninsula, *Earth Planet. Sci. Lett.*, *259*(3–4), 256–265, doi:10.1016/j.epsl.2007.04.035.

Hirth, G. (2002), Laboratory constraints on the rheology of the upper mantle, *Rev. Mineral. Geochem.*, *51*(1), 97–120, doi:10.2138/gsrmg.51.1.97.

Hirth, G., and D. Kohlstedt (2003), Rheology of the upper mantle and the mantle wedge: A view from the experimentalists, in *Inside the Subduction Factory*, *Geophys. Monogr. Ser.*, vol. 138, edited by J. Eiler, pp. 83–105, AGU, Washington, D. C., doi:10.1029/138GM06.

Hofstetter, A., C. Dorbath, M. Rybakov, and V. Goldshmidt (2000), Crustal and upper mantle structure across the Dead Sea rift and Israel from teleseismic P wave tomography and gravity data, *Tectonophysics*, *327*(1–2), 37–59, doi:10.1016/S0040-1951(00)00161-X.

Huismans, R. S., and C. Beaumont (2002), Asymmetric lithospheric extension: The role of frictional plastic strain softening inferred from numerical experiments, *Geology*, *30*(3), 211–214, doi:10.1130/0091-7613(2002)030<0211:ALETRO>2.0.CO;2.

Kameyama, M., D. A. Yuen, and S.-I. Karato (1999), Thermal-mechanical effects of low-temperature plasticity (the Peierls mechanism) on the deformation of a viscoelastic shear zone, *Earth Planet. Sci. Lett.*, *168*(1–2), 159–172, doi:10.1016/S0012-821X(99)00040-0.

Karato, S.-I. (2008), *Deformation of Earth Materials: An Introduction to the Rheology of Solid Earth*, Cambridge Univ. Press, Cambridge, U. K.

Koulakov, I., and S. V. Sobolev (2006), Moho depth and three-dimensional P and S structure of the crust and uppermost mantle in the eastern Mediterranean and Middle East derived from tomographic inversion of local ISC data, *Geophys. J. Int.*, *164*(1), 218–235, doi:10.1111/j.1365-246X.2005.02791.x.

Koulakov, I., S. V. Sobolev, M. Weber, S. Oreshin, K. Wylegalla, and R. Hofstetter (2006), Teleseismic tomography reveals no signature of the Dead Sea Transform in the upper mantle structure, *Earth Planet. Sci. Lett.*, *252*(1–2), 189–200, doi:10.1016/j.epsl.2006.09.039.

Krienitz, M.-S., K. M. Haase, K. Mezger, P. van den Bogaard, V. Thiemann, and M. A. Shaikh-Mashail (2009), Tectonic events, continental intraplate volcanism, and mantle plume activity in northern Arabia: Constraints from geochemistry and Ar-Ar dating of Syrian lavas, *Geochem. Geophys. Geosyst.*, *10*, Q04008, doi:10.1029/2008GC002254.

Leloup, P. H., Y. Ricard, J. Battaglia, and R. Lacassin (1999), Shear heating in continental strike-slip shear zones: Model and field examples, *Geophys. J. Int.*, *136*(1), 19–40, doi:10.1046/j.1365-246X.1999.00683.x.

Mechie, J., K. Abu-Ayyash, Z. Ben-Avraham, R. El-Kelani, I. Qabbani, and M. Weber (2009), Crustal structure of the southern Dead Sea basin derived from project DESIRE wide-angle seismic data, *Geophys. J. Int.*, *178*(1), 457–478, doi:10.1111/j.1365-246X.2009.04161.x.

Mohsen, A., R. Kind, S. V. Sobolev, and M. Weber (2006), Thickness of the lithosphere east of the Dead Sea Transform, *Geophys. J. Int.*, *167*(2), 845–852, doi:10.1111/j.1365-246X.2006.03185.x.

Park, Y., A. A. Nyblade, A. J. Rodgers, and A. Al-Amri (2007), Upper mantle structure beneath the Arabian Peninsula and northern Red Sea from teleseismic body wave tomography: Implications for the origin of Cenozoic uplift and volcanism in the Arabian Shield, *Geochem. Geophys. Geosyst.*, *8*, Q06021, doi:10.1029/2006GC001566.

Park, Y., A. A. Nyblade, A. J. Rodgers, and A. Al-Amri (2008), S wave velocity structure of the Arabian Shield upper mantle from Rayleigh wave tomography, *Geochem. Geophys. Geosyst.*, *9*, Q07020, doi:10.1029/2007GC001895.

Petrunin, A. G., and S. V. Sobolev (2006), What controls thickness of sediments and lithospheric deformation at a pull-apart basin?, *Geology*, *34*(5), 389–392, doi:10.1130/G22158.1.

Petrunin, A. G., and S. V. Sobolev (2008), Three-dimensional numerical models of the evolution of pull-apart basins, *Phys. Earth Planet. Inter.*, *171*(1–4), 387–399, doi:10.1016/j.pepi.2008.08.017.

Pollack, H. N., S. J. Hurter, and J. R. Johnson (1993), Heat flow from the Earth's interior: Analysis of the global data set, *Rev. Geophys.*, *31*(3), 267–280, doi:10.1029/93RG01249.

Quennell, A. M. (1958), The structural and geomorphic evolution of the Dead Sea Rift, *Q. J. Geol. Soc.*, *114*(1–4), 1–24, doi:10.1144/gsjgs.114.1.0001.

Ranalli, G. (1995), *Rheology of the Earth*, Chapman and Hall, London.

Rutter, E. H., and K. H. Brodie (1988), The role of tectonic grain size reduction in the rheological stratification of the lithosphere, *Geol. Rundsch.*, *77*(1), 295–307, doi:10.1007/BF01848691.

Rybacki, E., and G. Dresen (2000), Dislocation and diffusion creep of synthetic anorthite aggregates, *J. Geophys. Res.*, *105*(B11), 26,017–26,036, doi:10.1029/2000JB900223.

Rybakov, M., V. Goldshmidt, and Y. Rotstein (1997), New regional gravity and magnetic maps of the Levant, *Geophys. Res. Lett.*, *24*(1), 33–36, doi:10.1029/96GL03617.

Schütz, F., B. Norden, A. Förster, and the DESIRE Group (2012), Thermal properties of sediments in southern Israel: A comprehensive data set for heat flow and geothermal energy studies, *Basin Res.*, doi:10.1111/j.1365-2117.2011.00529.x, in press.

Segev, A., M. Rybakov, V. Lyakhovsky, A. Hofstetter, G. Tibor, V. Goldshmidt, and Z. Ben Avraham (2006), The structure, isostasy and gravity field of the Levant continental margin and the southeast Mediterranean area, *Tectonophysics*, *425*(1–4), 137–157, doi:10.1016/j.tecto.2006.07.010.

Shalev, E., V. Lyakhovsky, and Y. Yechieli (2007), Is advective heat transport significant at the Dead Sea basin?, *Geofluids*, *7*(3), 292–300, doi:10.1111/j.1468-8123.2007.00190.x.

Shalev, E., D. Levitte, R. Gabay, and E. Zemach (2008), Assessment of geothermal resources in Israel, *Rep. GSI/29/2008*, Geol. Surv. of Isr., Jerusalem.

Shamir, G. (2006), The active structure of the Dead Sea Depression, in *New Frontiers in Dead Sea Paleoenvironmental Research*, edited by Y. Enzel, A. Agnon, and M. Stein, *Spec. Pap. Geol. Soc. Am.*, *401*, 15–32, doi:10.1130/2006.2401(02).

Skemer, P., and S.-I. Karato (2007), Effects of solute segregation on the grain-growth kinetics of orthopyroxene with implications for the deformation of the upper mantle, *Phys. Earth Planet. Inter.*, *164*(3–4), 186–196, doi:10.1016/j.pepi.2007.06.011.

Skemer, P., J. M. Warren, P. B. Kelemen, and G. Hirth (2009), Microstructural and rheological evolution of a mantle shear zone, *J. Petrol.*, *51*(1–2), 43–53, doi:10.1093/petrology/egp057.

Sobolev, S. V., A. G. Petrunin, Z. Garfunkel, and A. Y. Babeyko (2005a), Thermo-mechanical model of the Dead Sea Transform, *Earth Planet. Sci. Lett.*, *238*(1–2), 78–95, doi:10.1016/j.epsl.2005.06.058.

Sobolev, A. V., A. W. Hofmann, S. V. Sobolev, and I. K. Nikogosian (2005b), An olivine-free mantle source of Hawaiian shield basalts, *Nature*, *434*(7033), 590–597, doi:10.1038/nature03411.

Sobolev, A. V., S. V. Sobolev, D. V. Kuzmin, K. N. Malitch, and A. G. Petrunin (2009), Siberian meimechites: Origin and relation to flood basalts and kimberlites, *Russ. Geol. Geophys.*, *50*(12), 999–1033, doi:10.1016/j.rgg.2009.11.002.

Sobolev, S. V., A. V. Sobolev, D. V. Kuzmin, N. A. Krivolutskaya, A. G. Petrunin, N. T. Arndt, V. A. Radko, and Y. R. Vasiliev (2011), Linking mantle plumes, large igneous provinces and environmental catastrophes, *Nature*, *477*(7364), 312–316, doi:10.1038/nature10385.

Stern, R. J., and P. Johnson (2010), Continental lithosphere of the Arabian Plate: A geologic, petrologic, and geophysical synthesis, *Earth Sci. Rev.*, *101*(1–2), 29–67, doi:10.1016/j.earscirev.2010.01.002.

ten Brink, U. S., Z. Ben-Avraham, R. E. Bell, M. Hassouneh, D. F. Coleman, G. Andreasen, G. Tibor, and B. Coakley (1993), Structure of the Dead Sea pull-apart basin from gravity analyses, *J. Geophys. Res.*, *98*(B12), 21,877–21,894, doi:10.1029/93JB02025.

ten Brink, U. S., A. S. Al-Zoubi, C. H. Flores, Y. Rotstein, I. Qabbani, S. H. Harder, and G. R. Keller (2006), Seismic imaging of deep low-velocity zone beneath the Dead Sea basin and transform fault: Implications for strain localization and crustal rigidity, *Geophys. Res. Lett.*, *33*, L24314, doi:10.1029/2006GL027890.

Thatcher, W., and P. C. England (1998), Ductile shear zones beneath strike-slip faults: Implications for the thermomechanics of the San Andreas fault zone, *J. Geophys. Res.*, *103*(B1), 891–905, doi:10.1029/97JB02274.

Weber, M., et al. (2004), The crustal structure of the Dead Sea Transform, *Geophys. J. Int.*, *156*(3), 655–681, doi:10.1111/j.1365-246X.2004.02143.x.

Weber, M., et al. (2009), Anatomy of the Dead Sea Transform from lithospheric to microscopic scale, *Rev. Geophys.*, *47*, RG2002, doi:10.1029/2008RG000264.